

Characterization of vacuum-evaporated ZnSe thin films

S. Venkatachalam^a, Y.L. Jeyachandran^a, P. Sureshkumar^a, A. Dhayalraj^a,
D. Mangalaraj^{a,*}, Sa.K. Narayandass^a, S. Velumani^b

^a Thin film laboratory, Department of Physics, Bharathiar University, Coimbatore-641046, India

^b Departamento de Fisica, ITESM-Campus, Monterrey, Nuevo Leon, C.P.64849, Mexico

Received 22 June 2006; received in revised form 11 October 2006; accepted 16 November 2006

Abstract

ZnSe thin films were prepared at different thicknesses using a vacuum evaporation technique under a vacuum of 3.9×10^{-8} bar. The composition, structure, optical and electrical properties of the deposited ZnSe thin films were studied using the energy dispersive X-ray analysis (EDAX), X-ray diffraction (XRD), optical transmittance and current–voltage measurements. The composition of the deposited films was found to be Zn (34.35%) and Se (65.65%). SEM images of ZnSe films on glass substrates revealed the smooth surface of the deposited films. X-ray analysis showed that the films deposited at a lower thickness were amorphous in nature, whereas at higher thicknesses, the films were crystalline in nature. The XRD patterns for higher thickness films exhibited reflections corresponding to the cubic (111) phase ($2\theta=27.33^\circ$). The values of the estimated energy gap from optical studies for amorphous films were greater than that obtained for crystalline ZnSe ($E_g=2.7$ eV) films. In the dc conduction studies, the free carrier mobility (μ_p), carrier density (p_0) and trap density values were calculated as $9.1738 \times 10^{-15} \text{ m}^2 \text{ V}^{-1} \text{ s}^{-1}$, $1.068 \times 10^{23} \text{ m}^{-3}$ and $4.2733 \times 10^{22} \text{ m}^{-3}$, respectively.

© 2006 Elsevier Inc. All rights reserved.

Keywords: Thin films; Composition; Structure; Optical transmission; I–V

1. Introduction

The growth of the group of II–VI compound semiconductors has attracted considerable attention due to their novel physical properties and wide range of applications in optoelectronic devices. II–VI compound semiconductors such as sulphides (S), selenides (Se) and tellurides (Te) of cadmium (Cd), zinc (Zn), mercury (Hg) are of interest as high-refractive-index materials in multilayer optical coatings since they all

have low absorption over a broad wavelength range. They are now widely used for the preparation of semiconductive elements. The II–VI group compounds semiconductor films have not only figured prominently for many years in a wide variety of commercial electronic applications, but they also have played an important role in the development of semiconductor device physics. Among these materials, ZnSe thin films have attracted considerable interest over the years owing to their wide range of applications in various optoelectronic devices and in solar cells. ZnSe has a direct bandgap of 2.7 eV and is transparent over a wide range of the visible spectrum. More progress has been achieved in the fabrication of blue-green light emitting

* Corresponding author. Tel.: +91 422 2425458; fax: +91 422 2422387.

E-mail address: dmraj800@yahoo.com (D. Mangalaraj).

diodes [1], photodiodes [2] and solar cells [3]. The deposition techniques employed for the preparation of thin films include evaporation [4], a chemical solution reduction process [5], electro-deposition [6] and sol–gel [7]. The present study is on vacuum evaporated ZnSe thin films. In this paper, we report the composition, structural, optical and electrical properties of vacuum evaporated ZnSe thin films.

2. Experimental techniques

Iodine doped ZnSe alloy has been prepared from its own constituent elements. Appropriate weights of Zn, Se and iodine (99.999% Balzers, Switzerland) were taken in a quartz tube and sealed under a vacuum of 1.3×10^{-3} Pa. The temperature of the furnace was raised gradually to 875 °C and left at this temperature for about 32 h and then, the ampoule was slowly cooled to room temperature. The ZnSe ingot was taken out from the ampoule and made into fine powder and used for evaporation. Zinc selenide thin films were prepared onto well-cleaned glass substrates using a vacuum evaporation technique under a vacuum of 3.9×10^{-8} bar. A top aluminium counter electrode was evaporated to form the Al–ZnSe–Al sandwich structure. The completed capacitor had an active area of about 5.38×10^{-6} m². Thicknesses of the films were measured using a multiple beam interference (Fizeau fringes) method and the thicknesses of the deposited films were found to be in the range from 70 to 130 nm. The surface morphology of the film was studied by SEM [JEOL, JSM 6400].

2.1. Structural properties

A structural analysis of the films has been made by using an X-ray diffractometer (Philips PW 1700, $\text{Cu K}\alpha$ radiation at $\lambda = 1.54056$ Å) in the 2θ range 10° to 70° . The particle size is calculated from the Scherrer formula:

$$D = \frac{0.94\lambda}{\beta \cos\theta} \quad (1)$$

where λ is the wavelength of the X-rays used, 2θ is the angle between the incident and scattered X-rays, and β is the full width at half maximum. The dislocation density (δ) is defined as the length of dislocation lines per unit volume of the crystal and is given by:

$$\delta = \frac{1}{D^2} \quad (2)$$

where D is the particle size and the strain (ε) value is calculated from the following relation:

$$\varepsilon = \left[\frac{\lambda}{D \cos\theta} - \beta \right] \frac{1}{\tan\theta} \quad (3)$$

The lattice spacing d is calculated using the Bragg relation:

$$d = \lambda / 2 \sin\theta \quad (4)$$

where λ is the wavelength of the X-rays used and the lattice parameter is calculated using the formula:

$$\frac{1}{d^2} = \frac{h^2 + K^2 + l^2}{a^2} \quad (5)$$

where h , k and l are miller indices of the lattice planes.

2.2. Optical properties

Optical transmission of ZnSe films deposited onto micro-glass slide was recorded using a UV-VIS-NIR Spectrophotometer (CARY 2390). The extinction coefficient can be calculated from the formula:

$$k = \frac{\ln\left(\frac{1}{T}\right)\lambda}{4\pi t} \quad (6)$$

where t is the thickness of the deposited film. The absorption coefficient can be calculated from the following relation:

$$\alpha = \frac{4\pi k}{\lambda} \quad (7)$$

The nature of the transition can be investigated on the basis of the dependence of the absorption coefficient with the incident photon energy $h\nu$. For direct and indirect allowed transitions, the theory of fundamental absorption leads to the following photon energy dependence near the absorption edge:

$$\alpha \propto (h\nu - E_g)^m \quad (8)$$

where $h\nu$ and E_g are the photon and the bandgap energy, respectively. In this relation, the values of m are 1/2 and 2 for direct allowed and indirect allowed transitions, respectively. The current across the capacitor as a function of the applied voltage from a dc power supply was measured in a vacuum of 1.3×10^{-3} Pa at different temperatures (300–395 K) using a cryostat equipped with a PT100 thermocouple.

3. Results and discussion

3.1. Composition and surface analysis

The films were deposited at different thicknesses (70, 100 and 130 nm). Composition of the deposited films was measured using EDAX analysis. Fig. 1 shows the EDAX spectrum of the deposited film (70 nm). The composition of the sample was calculated as Zn (34.35%) and Se (65.65%). The iodine concentration was found to be negligible. Fig. 2 shows SEM images of the films deposited at different thicknesses ($a=100$ nm and $b=130$ nm). The SEM images of ZnSe films on glass substrates revealed that the deposited films possess a smooth surface.

3.2. Structural properties

The vacuum evaporated ZnSe films were found to be uniform, smooth and having good adhesion with the substrate surface. Typical diffraction patterns of ZnSe films deposited on glass substrates at room temperature are shown in Fig. 3. The structure of the ZnSe films was found to be amorphous for lower thicknesses [$d=70$ to 100 nm] as shown in Figs. 3(a) and (b). At a higher thickness [$d=130$ nm], the films were found to be crystalline as depicted in Fig. 3(c). The deposited films of thickness 130 nm have a strong preferred orientation and only one intense peak was observed [8]. The observed lattice spacing ($d=3.264$ Å) value coincided with the standard JCPDS for cubic ZnSe. The XRD patterns [Fig. 3(c)] for higher thickness films exhibited reflections corresponding to the cubic phase i.e. $2\theta=27.33^\circ$, corresponding to the (111) plane of the cubic phase. Similar results have been reported by Pradip et al. [9]. The particle size (D), strain (ϵ), and dislocation density

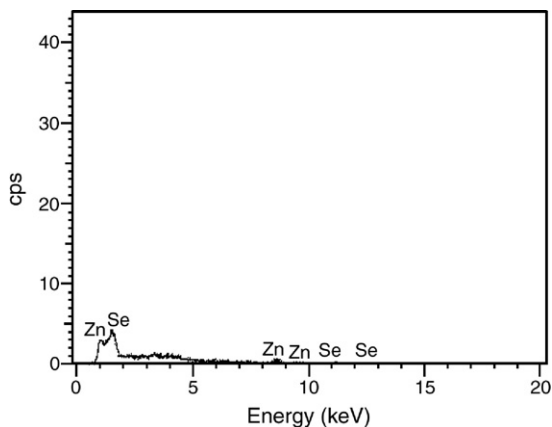


Fig. 1. EDAX spectrum of ZnSe thin films of 70 nm thickness.

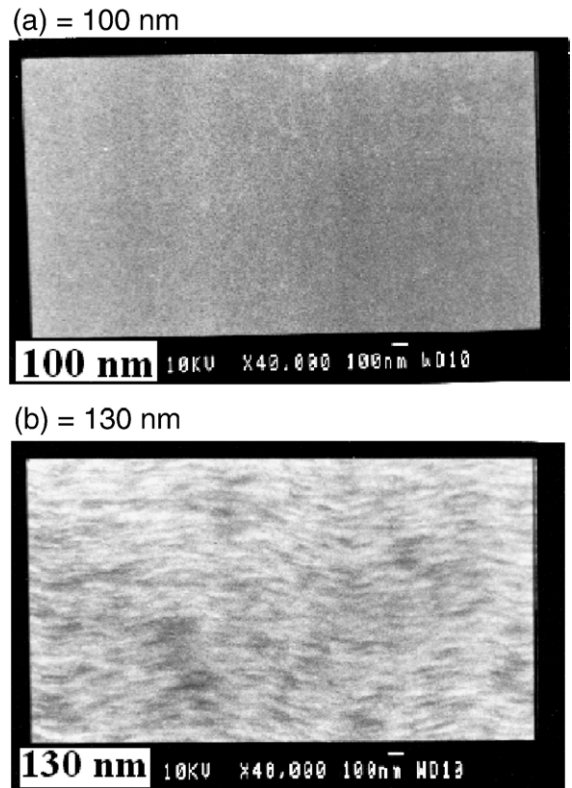


Fig. 2. SEM images of ZnSe thin films deposited at different thicknesses ($a=100$ nm and $b=130$ nm).

(δ) values were calculated as 16.34×10^{-9} nm, $2.39 \times 10^{-3} \text{ lin}^{-2} \text{ m}^{-4}$, and $3.74 \times 10^{15} \text{ lin m}^2$.

3.3. Optical properties

The optical transmittance spectra of ZnSe film for various thicknesses are shown in Fig. 4. Figs. 5(a)–(c)

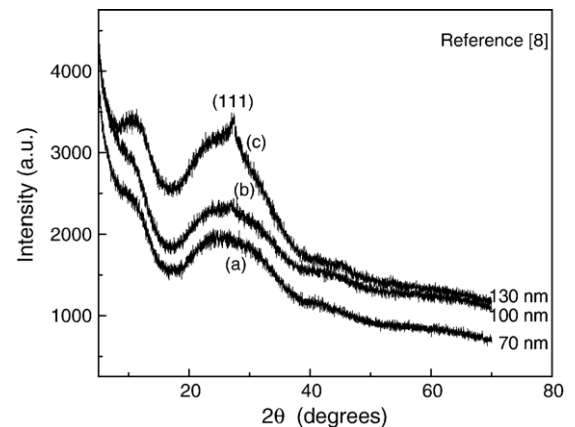


Fig. 3. X-ray diffractograms of ZnSe thin films deposited on glass substrates.

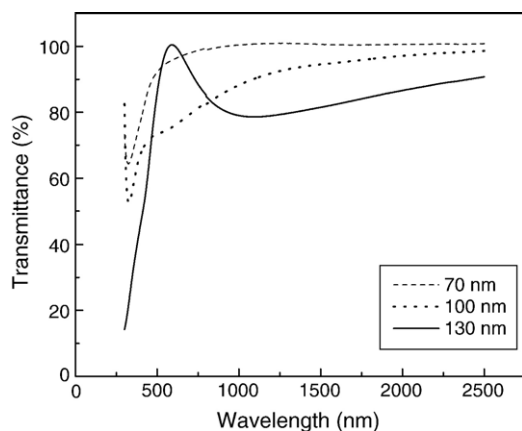


Fig. 4. Transmittance spectra of ZnSe thin films deposited at different thicknesses ($t=70, 100$ and 130 nm).

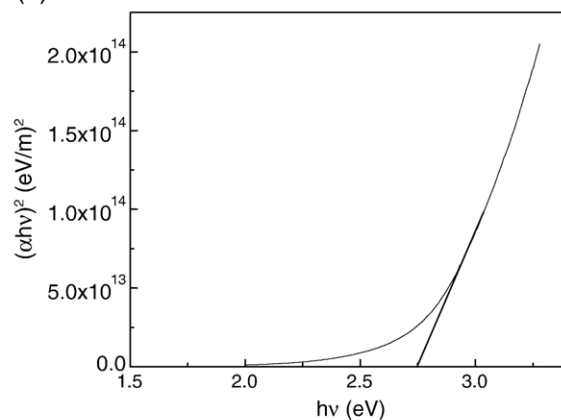
show the plot between $(\alpha h\nu)^2$ and $h\nu$ for various thicknesses ($t=70, 100$ and 130 nm). Extrapolation of the linear portion of the curve to $(\alpha h\nu)^2=0$ gives the optical band gap value for the deposited film. The calculated band gap (E_g) energies were 2.7 eV for crystalline ZnSe (direct transition) and 2.74 eV for amorphous ZnSe. The values of the estimated energy gap for amorphous films are greater than that obtained for crystalline ZnSe ($E_g=2.7$ eV) films, because in the polycrystalline material the electron transition is from band to band. On the other hand, in amorphous materials the electron transitions may be either from localized states at the valance band edge to extended states in the conduction band or from extended states in the valance band to the localized states at the conduction edge. This leads to higher energies than those for polycrystalline materials. The energy gaps of the films were found to lie in the range between 2.7 and 2.74 eV. Similar results have been reported by Riveros et al. [6]. The energy band gap value was found to decrease with an increase in film thickness and the films are found to have a direct allowed transition, which is in accordance with the energy band model of ZnSe films. The optical band gap value decreases with an increase in film thickness and this is likely to be attributed to an increase of particle size and decrease in strain values.

3.4. DC conduction studies

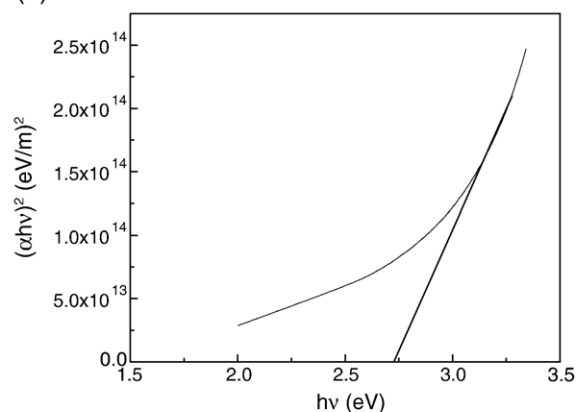
The current–voltage characteristics of ZnSe thin film of thickness 100 nm are shown in Fig. 6. Three regions are observed in the V versus I curve. In the first region, at low voltages (up to 5 V), the conduction is Ohmic ($I \propto V$). In the second region i.e. the voltage range between 5 and 6.1 V, a trap square law ($I \propto V^2$) dependence is observed.

In the third region (>6.1 V), the conduction mechanism is a space charge limited current (SCLC) mechanism. The growth of current faster than V^2 after the square law region is strongly temperature dependent suggesting that

(a) = 70 nm



(b) = 100 nm



(c) = 130 nm

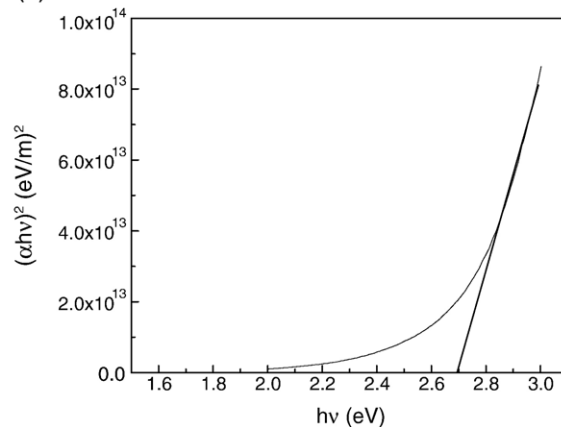


Fig. 5. (a–c) The plot of $(\alpha h\nu)^2$ versus $h\nu$ of the ZnSe thin film deposited at different thicknesses ($t=70, 100$ and 130 nm).

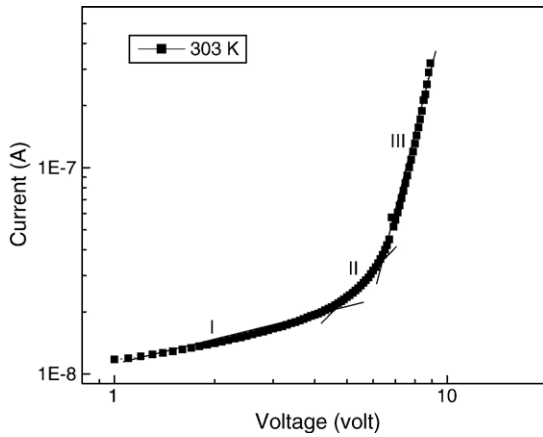


Fig. 6. Current versus voltage curve of Al–ZnSe–Al sandwich thin film capacitor.

the dominant trapping level lies above the Fermi level [10]. This reveals the prevalence of a space charge conduction mechanism in the Al–ZnSe–Al thin film capacitor. The relation for the current density in the square law region is [11]:

$$J = \frac{9}{8} \mu_p \varepsilon' \varepsilon_0 \theta \frac{V^2}{t^3} \quad (9)$$

where μ_p is the hole mobility, ε_0 is the permittivity of free space and ε' is the dielectric constant of the material of the film. The shallow trapping level is defined as a level, above the Fermi level in the material. So the Fermi level in high resistivity materials must lie near the center of the band gap and these trap levels are in a position normally referred to as “deep”. For the case of hole injection and hole trapping θ is given by the equation [10]:

$$\theta = \frac{N_c}{N_t} \exp\left(\frac{-E_t}{kT}\right) \quad (10)$$

where N_c is the effective density of states in the conduction band edge, N_t is the density of shallow traps positioned at an energy E_t below the conduction band, k is the Boltzmann constant, T is the temperature, θ is the ratio between the free hole density (p_0) in the conduction band to the total electron density ($p_0 + p_1$), p_1 being the trapped hole density and p_0 is the free hole density. Experimentally, θ is the ratio of the current density I_1/A at the beginning of the square law region to the current density I_2/A at the end of the square law region, where A is the area of the capacitor:

$$\frac{I_1}{I_2} = \theta = \frac{p_0}{p_0 + p_1} \quad (11)$$

Using the experimental value of θ and $\varepsilon' = 9.14$ in Eq. (9), the free carrier mobility value is calculated as $9.1738 \times 10^{-15} \text{ m}^2 \text{ V}^{-1} \text{ s}^{-1}$. The estimated mobility value is very low compared with the reported value for pure bulk ZnSe. Therefore these results indicate that the carrier mobilities in ZnSe thin films which contain contamination by iodine atoms are influenced by the carrier scattering at the microcrystalline boundaries [12]. The equilibrium concentration of charge carriers in the conduction band is calculated from the relation:

$$p_0 = \frac{\varepsilon' \varepsilon_0 \theta}{qt^2} V_{tr} \quad (12)$$

Here V_{tr} is the value at which the transition from the Ohmic to square law region takes place, q is the electronic charge and t is the thickness of the film. The value of the free carrier density (p_0) is calculated as $1.068 \times 10^{23} \text{ m}^{-3}$. From Eq. (11), the trap density value is calculated as $4.2733 \times 10^{22} \text{ m}^{-3}$.

4. Conclusions

In the present study, ZnSe thin films of different thicknesses were deposited onto glass substrates under a vacuum of $3.9 \times 10^{-3} \text{ Pa}$ using a vacuum evaporation technique. The composition of the deposited film was calculated as Zn (34.35%) and Se (65.65%). X-ray analysis showed that the film deposited at lower thickness has an amorphous nature and at higher thicknesses the films were crystalline in nature. From the optical transmittance spectra, it is evident that the films have good transmittance in the higher wavelength region. The band gap values were found to decrease with an increase of film thickness, which could be attributed to an increase in particle size and decrease in strain values. An Al–ZnSe–Al sandwich thin film capacitor was fabricated. SCLC conduction was used as a useful tool for the evaluation of the electrical parameters of ZnSe films. In the d.c. conduction studies, the conduction mechanism was found to be space charge limited.

References

- [1] Shirakawa Tsuguru. Effect of defects on the degradation of ZnSe-based white LEDs. Mater Sci Eng, B, Solid-State Mater Adv Technol 2002;91–92:470–5.
- [2] de Melo O, Santana G, Melendez-Lira M, Hernandez-Calderon I. Observation of the photovoltaic effect in n-ZnSe/p-GaAs heterostructures. J Cryst Growth 1999;201–202:971–4.
- [3] Bohne W, Lindner S, Rohrich J. Study of In diffusion into ZnSe buffer-layer material of chalcopyrite solar cells with rough

- surfaces by means of ERDA measurements. *Nucl Instrum Methods B* 2002;188:55–60.
- [4] Khawaja EE, Durrani SMA, Hallak AB, Salim MA, Sakhawah Hussain M. Density of thin vapour-deposited films of zinc selenide. *J Phys D; Appl Phys* 1994;27:1008–13.
- [5] Wang C, Qian XF, Zhang WX, Zhang XM, Xie Y, Qian YT. Preparation of ZnSe films through chemical solution reduction process. *Mater Res Bull* 1999;34(10–11):1637–41.
- [6] Riveros G, Gomez H, Henriquez R, Schrebler R, Marotti RE, Dalchide EA. Electrodeposition and characterization of ZnSe semiconductor thin films. *Sol Energy Mater Sol Cells* 2001;70:255–68.
- [7] Li Guangming, Nogami Masayuki. Preparation and optical properties of sol–gel derived ZnSe crystallites doped in glass films. *J Appl Phys* 1994;75(8):4276–8.
- [8] JCPDS, X-ray powder diffraction file, Joint Committee for Powder Diffraction.
- [9] Kalita Pradip KR, Sarma BK, Das HC. Structural characterization of vacuum evaporated ZnSe thin films. *Bull Mater Sci* 2000;23(4):313–7.
- [10] Lampert MA, Mark P. *Current Injection in Solids*. New York: Academic Press; 1970.
- [11] Basol BM, Stafudd DM. Observation of electron traps in electrochemically deposited CdTe films. *Solid State Electron* 1981;24:121–5.
- [12] Tominaga K, Takao T, Fukushima A, Moriga T, Nakabayashi I. Film properties of ZnO:Al films deposited by co-sputtering of ZnO:Al and contaminated Zn targets with Co, Mn and Cr. *Vacuum* 2002;66:511–5.